

Two-Pass Zero-Shot Temporal-Spatial Grounding of Rare Traffic Events in Surveillance Video

Jiantang Huang

huang.jiant@northeastern.edu

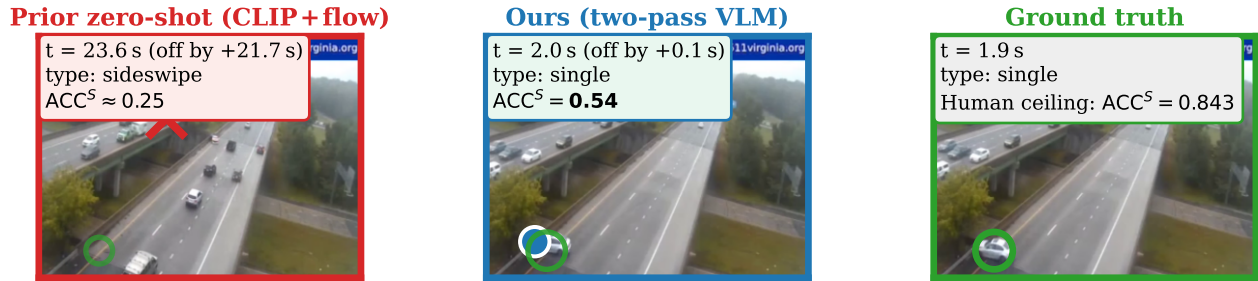


Figure 1. **Teaser.** On a real CCTV clip from ACCIDENT@CVPR 2026, the Kaggle optical-flow public baseline [11] picks a moment +21.7 s after the actual collision (traffic appears normal) with the wrong type; our two-pass VLM grounding recovers the impact to 0.1 s and correctly labels the *single*-vehicle roll-over. Green: ground truth, blue: ours, red: prior. We reach $ACC^S=0.539$, +0.127 over the benchmark paper’s best-of-baselines oracle [14] on ACCIDENT@CVPR 2026 without supervised training on labeled real accident videos.

Abstract

Grounding traffic accidents in real CCTV footage is a rare-event problem where training on labeled accident video is often prohibited, yet accurate joint localization in time, space, and collision type is required. We present a no-fine-tuning pipeline that elicits this joint output from frozen vision-language models through two ideas. First, a coarse-to-fine two-pass decomposition: a full-video pass at 1 fps produces a coarse (t, x, y, c) tuple, then a second pass at 5 fps within a ± 3 s window refines time and location, with two deterministic confidence gates that revert to the coarse estimate on boundary hedges or edge-clamped coordinates. Second, a specialist role assignment: Qwen3-VL-Plus handles grounding, Gemini 3.1 Flash-Lite handles typing on a centered video clip. On the ACCIDENT@CVPR 2026 benchmark (2,027 real CCTV videos) we reach $ACC^S=0.539$ (95% CI [0.525, 0.553]): +0.127 over the benchmark paper’s best-of-baselines oracle (0.412), +0.143 over the strongest single-VLM baseline (Molmo-7B, 0.396), and +0.250 over the naive baseline (0.289) [14]. The VLM path uses up to three API calls per video (17% fall back to physics on API failures); the full run costs $\sim \$20$. We further diagnose a +1.55 s late bias in VLM temporal grounding, length-dependent degradation, and a physics-VLM oracle reaching 2.13 s temporal MAE, outlining concrete next steps.

1. Introduction

Traffic accidents are rare, safety-critical events: the payoff for automatic detection from CCTV is high, yet labeled accident footage at the volume needed for modern supervised recognition is difficult to obtain, and privacy and liability concerns often forbid training on real incidents. The ACCIDENT@CVPR 2026 benchmark [14] encodes exactly this regime – 2,211 CARLA synthetic videos for development and 2,027 real CCTV clips for test, with a blanket prohibition on training on real accident video. Each clip must be grounded jointly in time, space, and collision type, and systems are scored by the harmonic mean ACC^S of the three subtask scores.

The harmonic-mean protocol punishes weak components. Official Kaggle public-baseline notebooks [11] (Optical Flow, BBox Dynamics) score $ACC^S=0.251$ and 0.270 – below the naive 0.289 [14]. The strongest single-VLM (Molmo-7B [4], 0.396) excels at spatial ($S=0.596$) but fails on type ($C=0.271$); the benchmark paper’s best-of-baselines oracle reaches 0.412; human is 0.843. Closing this gap without training requires moving beyond hand-crafted primitives and single-shot VLM prompting.

Our starting observation is that modern vision-language models – Qwen3-VL-Plus [1] and Gemini 3 [7] – already ship native spatio-temporal grounding: textual timestamp alignment, $[0, 1000]^2$ coordinate outputs, and long-context video windows. Naive zero-shot use of these models still

underperforms, for two reasons visible in the data. A single forward pass over a whole video must choose between coarse temporal coverage and fine temporal resolution; and any single VLM is typically strongest on only a subset of the three subtasks. We address both with a coarse-to-fine two-pass decomposition that refines only the high-salience neighborhood, and a specialist role assignment that hands typing to a second VLM whose video classifier outperforms the grounding model on this axis.

Contributions. (i) A no-fine-tuning coarse-to-fine two-pass VLM grounding pipeline with deterministic temporal and spatial confidence gates, in contrast to the *trained* hierarchical grounding of [9]. (ii) A specialist role split – Qwen3-VL for $T+S$, Gemini 3.1 for C – lifting full-test type accuracy from 0.474 to 0.591 (+25% relative). (iii) A systematic failure analysis: +1.55 s late bias, length-dependent degradation, and a physics-VLM oracle at 2.13 s MAE (−33.5%). (iv) On ACCIDENT@CVPR 2026, $ACC^S=0.539$ (CI [0.525, 0.553]): +0.127 over the benchmark paper’s best-of-baselines oracle [14] and +0.143 over the best single-VLM (Molmo-7B [4], 0.396), at ~\$20 API cost.

2. Related Work

Traffic accident detection from video has a decade-long history, spanning supervised CCTV classification (CADP [15], TAD [21]), unsupervised detection on dashcams (DoTA [22]), and anticipation with spatio-temporal attention (DSTA [12], CCD [2]); a recent survey catalogs the field [5]. These works almost universally train on labeled accident footage. The ACCIDENT@CVPR 2026 challenge [14] breaks this assumption: 2,211 CARLA synthetic videos are provided for development, but the 2,027-video real CCTV test set forbids training on real accidents. Concurrent with our work, Thakur and Talele [16] propose a modular zero-shot pipeline (frame-difference peaks for time, Farneback flow centroid for space, CLIP similarity for type), reaching $ACC^S=0.252$.

VLM temporal grounding has progressed rapidly with trained video LLMs. VTimeLLM [10], TRACE [8], and Grounded-VideoLLM [18] introduce timestamp tokens, causal event modeling, or two-stream encoders – all fine-tuned on dedicated video-temporal-grounding corpora. RevisionLLM [9] is closest in spirit to our method, applying recursive coarse-to-fine grounding on hour-long videos, but its hierarchy is realized through hierarchical *training*. Qwen3-VL [1] and Gemini 3 [7] ship native spatio-temporal grounding (object-level video tracks, textual timestamp alignment), opening the door to training-free use.

Zero-shot / training-free rare-event localization and anomaly detection is dominated by CLIP-style adapters – AnomalyCLIP [24], VadCLIP [20] – which still require auxiliary anomaly data or weak labels. LAVAD [23] is the first fully training-free VAD pipeline, but relies on frame-

by-frame VLM captioning and LLM post-aggregation, losing spatial grounding. Hierarchical video systems such as VideoTree [19] and VideoMiner [3] focus on long-video QA rather than precise $T+S+C$ rare-event outputs. Grounding VLMs – Molmo [4], SigLIP 2 [17], DINOv2 [13] – excel at pointing but typically treat time implicitly.

Our method combines three choices: (i) training-free, using only frozen VLMs; (ii) two-pass coarse-to-fine native VLM grounding rather than separate captioning-then-LLM or trained hierarchy; and (iii) specialist role assignment across two VLMs.

3. Method

3.1. Pipeline Overview

Given a traffic surveillance video V of duration D seconds, we predict (t^*, x^*, y^*, c^*) with $t^* \in [0, D]$, $(x^*, y^*) \in [0, 1]^2$ (Qwen3-VL emits raw coordinates on a $[0, 1000]^2$ grid; we divide by 1000 before merging and evaluation), and $c^* \in \mathcal{C} = \{\text{head-on, rear-end, t-bone, sideswipe, single}\}$. The ACCIDENT@CVPR 2026 protocol forbids training on real accident footage; the main path uses frozen VLMs, and API failures fall back to a frozen-detector + rule-based physics module. Fig. 2 shows the three stages. A first pass over V with Qwen3-VL-Plus [1] produces a coarse tuple (t_1, x_1, y_1, c_1) at 1 fps. A second pass on a ± 3 s window around t_1 , sampled at 5 fps and 1024 px, refines time and location to (t_2, x_2, y_2) . A deterministic merge reconciles the two spatial estimates, and a Gemini 3.1 Flash-Lite [6] classifier re-labels type from a short clip centered on t^* . Three design choices drive the method: (i) coarse-to-fine decomposition exploiting native VLM grounding without fine-tuning (unlike [9]); (ii) confidence-driven fallback accepting Pass 2 only when it passes temporal and spatial sanity checks; (iii) specialist role assignment across two VLMs ([23] uses a single captioner). Alg. 1 gives the full procedure; total inference cost on the 2,027 test videos is ~\$20 (~\$0.01 per video).

3.2. Pass 1: Coarse Grounding

Pass 1 samples V at 1 fps, ≤ 30 frames, 720 px long edge (median ACCIDENT clip is 26.8 s). Frames are serialized into one multimodal message, each prefixed by a `[Frame at t.ts]` tag that binds the pixel grid to its absolute second – a lightweight anchor Qwen3-VL reads directly, avoiding trained time-to-token modules [8, 10]. The prompt declares up-front that *an accident occurs* (closed-world framing that discourages refusals; this matches the ACCIDENT benchmark where every clip contains an accident, and bounds open-world deployment to a human-in-the-loop gate, App. F), asks for the impact second, a point in $[0, 1000]^2$ (Qwen3-VL’s native grounding convention [1]), and a class in \mathcal{C} with one-line visual definitions. The combination of

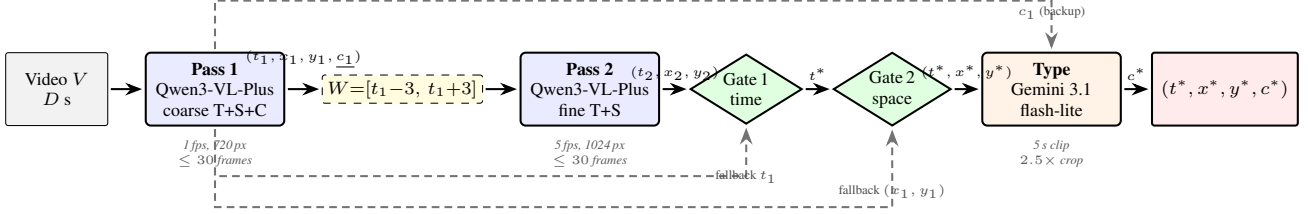


Figure 2. **Two-pass zero-shot grounding pipeline with two confidence gates.** Pass 1 (Qwen3-VL-Plus) produces a coarse tuple from 1 fps frames of the full video; c_1 is struck through on the main path because type is re-assigned to Gemini, but retained as a backup if the Gemini call fails. Pass 2 refines time and location on a ± 3 s window sampled at 5 fps and 1024 px. **Gate 1** (temporal fallback) keeps t_1 when Pass 2 returns -1 or a time near the window boundary; otherwise $t^* \leftarrow t_2$. **Gate 2** (spatial merge) keeps (x_2, y_2) only when both axes lie in $[10, 990]$ on the $[0, 1000]^2$ grid; otherwise (x_1, y_1) . A specialist Gemini 3.1 Flash-Lite Preview classifier re-labels type on a 5 s clip centered on t^* . All models are frozen and used zero-shot.

1 fps sampling, integer-second output, and per-frame textual tags turns temporal localization into naming a specific frame rather than producing a continuous timestamp. On API failure (17% of videos in practice), we fall back to a parallel YOLO26x + ByteTrack + physics pipeline (pair- and single-vehicle scoring, rule-based type); all other videos are processed end-to-end by VLMs.

3.3. Pass 2: Fine Refinement and Merge

Pass 2 re-samples V at 5 fps inside $W = [\max(0, t_1 - 3), \min(D, t_1 + 3)]$, yielding ≤ 30 frames at 1024 px, each tagged with its fractional timestamp. The prompt asks for 0.1 s precision and a fresh point in $[0, 1000]^2$, and explicitly allows $t_2 = -1$ if no collision is visible within W . This escape hatch turns Pass 2 into a *confidence-gated refiner* rather than a naive overwrite.

Temporal fallback (Gate 1). With boundary tolerance $\tau = 0.3$ s,

$$t^* = \begin{cases} t_1 & t_2 < 0 \text{ or } |t_2 - W_{\min}| < \tau \\ & \text{or } |t_2 - W_{\max}| < \tau, \\ t_2 & \text{otherwise.} \end{cases} \quad (1)$$

Eq. 1 interprets a -1 response or a boundary-adjacent time as low-confidence hedging and falls back to the more robust Pass 1 estimate.

Spatial merge (Gate 2). A deterministic post-processing step reconciles the two spatial estimates. Let $(\tilde{x}_1, \tilde{y}_1)$ and $(\tilde{x}_2, \tilde{y}_2)$ denote the raw Pass 1 and Pass 2 coordinates on the $[0, 1000]^2$ grid. With margin $m = 10$,

$$(x^*, y^*) = \begin{cases} (\tilde{x}_2/1000, \tilde{y}_2/1000) & m \leq \tilde{x}_2 \leq 1000 - m \text{ and} \\ & m \leq \tilde{y}_2 \leq 1000 - m, \\ (\tilde{x}_1/1000, \tilde{y}_1/1000) & \text{otherwise.} \end{cases} \quad (2)$$

All four axis conditions must hold; if any axis is edge-clamped we revert to the Pass 1 coordinate. The two gates (Eq. 1, 2) form independent confidence checks that let the two passes outperform either alone (§4.3).

Algorithm 1 TWOPASSGROUND: zero-shot T+S+C grounding.

Require: Video V of duration D ; VLMs $\mathcal{M}_Q, \mathcal{M}_G$; window $\Delta = 3$ s; tolerance $\tau = 0.3$ s; margin $m = 10$.

Ensure: (t^*, x^*, y^*, c^*) .

- 1: $F_1 \leftarrow \text{SAMPLE}(V, 1 \text{ fps}, 720 \text{ px}, \leq 30)$
- 2: $(t_1, \tilde{x}_1, \tilde{y}_1, c_1) \leftarrow \mathcal{M}_Q(F_1, \pi_{\text{coarse}})$; raw $[0, 1000]^2$
- 3: $W \leftarrow [\max(0, t_1 - \Delta), \min(D, t_1 + \Delta)]$
- 4: $F_2 \leftarrow \text{SAMPLE}(V|_W, 5 \text{ fps}, 1024 \text{ px}, \leq 30)$
- 5: $(t_2, \tilde{x}_2, \tilde{y}_2) \leftarrow \mathcal{M}_Q(F_2, \pi_{\text{fine}})$; on API failure $(-1, 0, 0)$ (absorbed by Gates 1 & 2)
- 6: // Gate 1: temporal fallback
- 7: **if** $t_2 < 0$ **or** $|t_2 - W_{\min}| < \tau$ **or** $|t_2 - W_{\max}| < \tau$ **then**
- 8: $t^* \leftarrow t_1$
- 9: **else**
- 10: $t^* \leftarrow t_2$
- 11: **end if**
- 12: // Gate 2: spatial merge
- 13: **if** $m \leq \tilde{x}_2 \leq 1000 - m$ **and** $m \leq \tilde{y}_2 \leq 1000 - m$ **then**
- 14: $(x^*, y^*) \leftarrow (\tilde{x}_2/1000, \tilde{y}_2/1000)$
- 15: **else**
- 16: $(x^*, y^*) \leftarrow (\tilde{x}_1/1000, \tilde{y}_1/1000)$
- 17: **end if**
- 18: $C \leftarrow \text{CROPCLIP}(V, t^*, (\tilde{x}_1/1000, \tilde{y}_1/1000), [t^* - 3, t^* + 2], 2.5 \times)$
- 19: $c^* \leftarrow \mathcal{M}_G(C, \pi_{\text{type}})$; on failure $c^* \leftarrow c_1$
- 20:
- 21: **return** (t^*, x^*, y^*, c^*)

3.4. Specialist Type Classification

Qwen3-VL’s type accuracy is 0.462 on the 1,681 Pass-1-valid videos (full-test $C = 0.474$ including the 17% physics fallback), well below its spatial score, so we reassign typing to a second VLM. A 5 s clip spanning $[t^* - 3, t^* + 2]$ is extracted, spatially cropped around the Pass 1 center (x_1, y_1) at $2.5 \times$ box, and passed to gemini-3.1-flash-lite-preview with a closed-world prompt that enumerates \mathcal{C} and forbids abstention. On API failure we fall back to c_1 . We crop around the Pass-1 center (x_1, y_1) rather than the merged (x^*, y^*) because Pass 1 provides a more stable coarse region for type classifi-

Table 1. Main results on ACCIDENT (2,027 real CCTV videos), official evaluator at $\sigma_t=1$. Kaggle baselines [11]; Naive/Molmo-7B/Best-of-baselines/Human from [14]. T, S, C : dataset-level means; ACC^S : per-video HM averaged (leaderboard-reported for ours); CIs from 1,000 bootstrap resamples.

Method	T	S	C	ACC^S
Optical Flow [11]	—	—	—	.251
BBox Dynamics + OF [11]	—	—	—	.270
Naive baseline [14]	.30	.25	.34	.289
Molmo-7B [4]	.48	.60	.27	.396
Best-of-baselines [14]	.48	.60	.49	.412
Gemini 3.1 single-pass (ours)	.44	.49	.49	.473 [.46,.49]
Qwen3-VL Pass 1 (ours)	.46	.51	.47	.480 [.47,.49]
Ours (full)	.50	.54	.59	.539 [.53,.55]
Human [14]	.98	1.0	.92	.843

Table 2. Component ablation; T at $\sigma_t \in \{1, 2\}$, ACC^S at $\sigma_t=1$.

Configuration	T_{σ_1}	T_{σ_2}	S	C	ACC^S
Pass 1 only (Qwen type)	0.463	0.614	0.506	0.474	0.480
+ Gemini type	0.463	0.614	0.506	0.590	0.514
+ Pass 2 time	0.497	0.626	0.506	0.591	0.528
+ Pass 2 spatial	0.497	0.626	0.538	0.591	0.539

cation. This split lifts full-test type accuracy from 0.474 to 0.591 (+25% relative) at one extra API call per video.

4. Experiments

4.1. Setup

We evaluate on the 2,027 real CCTV clips of ACCIDENT@CVPR 2026 with per-video (time, 2D center, type) annotations; test-split labels were released publicly post-competition with our hyperparameters frozen before release (App. B). Per [14], ACC^S is the per-video harmonic mean averaged over videos; reported T, S, C are dataset-level component means ($\neq 3/(1/T+1/S+1/C)$ in general). T : Gaussian at GT time ($\sigma_t=1$ s); S : anisotropic spatial Gaussian ($\sigma_x=0.127, \sigma_y=0.119$); C : top-1 type accuracy. Baselines: two Kaggle public notebooks [11], the benchmark paper’s naive, Molmo-7B, best-of-baselines oracle, and human ceiling [14].

4.2. Main Results

Our pipeline reaches $ACC^S=0.539$ (CI [0.525, 0.553]); +0.127 over the best-of-baselines oracle and +0.143 over Molmo-7B. $T=0.497$ exceeds Molmo’s; $S=0.538$ trails Molmo’s 0.596; $C=0.591$ is highest reported. *Gemini 3.1 alone* on the same 1 fps input scores only 0.473 [.46, .49], below our Qwen Pass 1 (0.480); paired bootstrap shows our pipeline beats Gemini-alone by $\Delta=+0.066$ ($p<0.001$). On the 1,681 Pass-1-valid videos $ACC^S=0.554$; the 346 fallback videos (App. D) score 0.457; naive-fill fallback yields 0.501, confirming the VLM pipeline drives the gain.

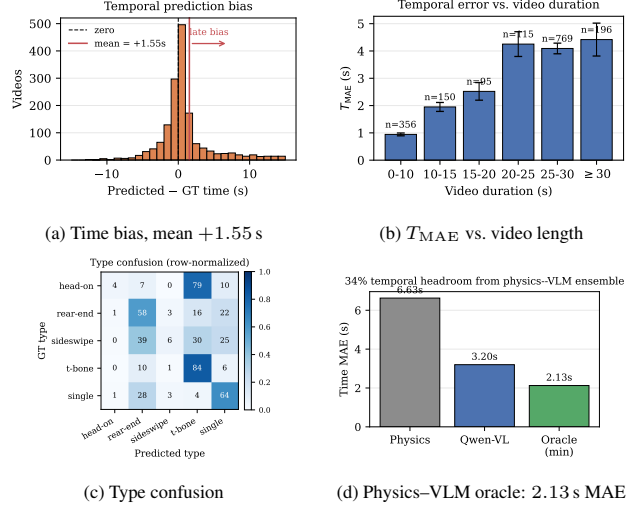


Figure 3. **Failure diagnostics.** (a) Pass 1 time is right-skewed, mean +1.55 s. (b) Temporal MAE grows with video length. (c) Head-on \rightarrow t-bone (79%), sideswipe \rightarrow rear-end (39%). (d) Oracle of YOLO+physics (6.63 s) and Qwen-Pass 1 (3.20 s) reaches 2.13 s (-33.5%).

4.3. Ablation

Table 2 decomposes the gain. Replacing Qwen’s type head with Gemini lifts C by +0.12 (largest single jump); Pass 2 time refinement adds +0.034 to $T(\sigma_t=1)$; Pass 2 spatial merge adds +7% to S . Cumulative gain over Pass 1 alone is +0.059 ACC^S .

4.4. Failure Mode Analysis

Temporal: late-bias + length. Pass 1 (predicted $-$ GT) time has mean +1.55 s, median +0.37 s (Fig. 3a): the VLM picks the post-collision wreckage frame, not contact. T_{MAE} also grows from 0.94 s on ≤ 10 s clips to > 4 s on ≥ 20 s clips (Fig. 3b), arguing for motion-adaptive sampling.

Type confusion. The confusion matrix (Fig. 3c) shows the two hardest classes collapsing: 79% of head-on is called t-bone, 39% of sideswipe is called rear-end. Per-type (App. E), head-on and sideswipe fall near $ACC^S=0.12$ from type alone $- T, S$ are healthy. The head-on \rightarrow t-bone collapse is plausibly driven by monocular depth ambiguity in high-angle CCTV and web-data label bias.

Physics-VLM oracle. On the 1,681 Pass-1-valid videos, an oracle of YOLO+physics (6.63 s) and Qwen-Pass 1 (3.20 s) reaches 2.13 s MAE (Fig. 3d, -33.5%).

4.5. Conclusion

Two-pass grounding plus a specialist VLM split achieves $ACC^S=0.539$ on ACCIDENT@CVPR 2026 (+0.127 over the benchmark paper’s best-of-baselines oracle, \sim \$20 cost). Next levers: adaptive sampling and physics-VLM fusion, not scale.

References

- [1] Jinze Bai et al. Qwen3-VL technical report. *arXiv preprint arXiv:2511.21631*, 2025. 1, 2, 6
- [2] Wentao Bao, Qi Yu, and Yu Kong. Uncertainty-based traffic accident anticipation with spatio-temporal relational learning. In *ACM MM*, 2020. 2
- [3] Xiangyu Cao et al. VideoMiner: Iteratively grounding key frames of hour-long videos via tree-based group relative policy optimization. In *ICCV*, 2025. 2
- [4] Matt Deitke et al. Molmo and PixMo: Open weights and open data for state-of-the-art vision-language models. In *CVPR*, 2025. 1, 2, 4
- [5] Jianwu Fang, Jiahuan Qiao, Jianru Xue, and Zhengguo Li. Vision-based traffic accident detection and anticipation: A survey. *IEEE TCSVT*, 2023. 2
- [6] Google. Gemini 3.1 Flash-Lite. <https://docs.cloud.google.com/vertex-ai/generative-ai/docs/models/gemini/3-1-flash-lite>, 2026. Vertex AI model documentation; generally available March 2026. The preview snapshot gemini-3.1-flash-lite-preview was used at submission time (April 2026). 2, 5, 6
- [7] Google DeepMind. Gemini 3 pro model card. <https://storage.googleapis.com/deepmind-media/Model-Cards/Gemini-3-Pro-Model-Card.pdf>, 2025. Model card, December 2025. Model family overview: <https://deepmind.google/models/gemini/>. 1, 2
- [8] Yongxin Guo et al. TRACE: Temporal grounding video LLM via causal event modeling. In *ICLR*, 2025. 2
- [9] Tanveer Hannan et al. ReVisionLLM: Recursive vision-language model for temporal grounding in hour-long videos. In *CVPR*, 2025. 2
- [10] Bin Huang, Xin Wang, Hong Chen, Zihan Song, and Wenwu Zhu. VTimeLLM: Empower LLM to grasp video moments. In *CVPR*, 2024. 2
- [11] Kaggle Competition Organizers. ACCIDENT @ CVPR 2026: Public baseline notebooks (optical flow $ACC^s=0.251$, bbox dynamics + of $ACC^s=0.270$). <https://www.kaggle.com/competitions/accident/code>, 2026. 1, 4, 6
- [12] Muhammad Monjurul Karim, Yu Li, Ruwen Qin, and Zhaozheng Yin. DSTA: A dynamic spatial-temporal attention network for early anticipation of traffic accidents. *arXiv preprint arXiv:2106.10197*, 2021. 2
- [13] Maxime Oquab, Timothée Darcet, Théo Moutakanni, Huy Vo, Marc Szafraniec, et al. DINOv2: Learning robust visual features without supervision. *Trans. Mach. Learn. Res.*, 2024. 2
- [14] Lukáš Pícek, Michal Čermák, Marek Hanzl, and Vojtěch Čermák. ACCIDENT: A benchmark dataset for vehicle accident detection from traffic surveillance videos. In *2025 IEEE/CVF Conference on Computer Vision and Pattern Recognition Workshops (CVPRW)*. IEEE, 2026. 1, 2, 4, 6
- [15] Ankit Parag Shah, Jean-Baptiste Lamare, Tuan Nguyen Anh, and Alexander Hauptmann. CADP: A novel dataset for CCTV traffic camera based accident analysis. In *AVSS*, 2018. 2
- [16] Amey Thakur and Sarvesh Talele. A modular zero-shot pipeline for accident detection, localization, and classification in traffic surveillance video. *arXiv preprint arXiv:2604.09685*, 2026. 2
- [17] Michael Tschannen et al. SigLIP 2: Multilingual vision-language encoders with improved semantic understanding, localization, and dense features. *arXiv preprint arXiv:2502.14786*, 2025. 2
- [18] Haibo Wang et al. Grounded-VideoLLM: Sharpening fine-grained temporal grounding in video large language models. In *Findings of EMNLP*, 2025. 2
- [19] Ziyang Wang et al. VideoTree: Adaptive tree-based video representation for LLM reasoning on long videos. In *CVPR*, 2025. 2
- [20] Peng Wu, Xuerong Zhou, Guansong Pang, Lingru Zhou, Qingsen Yan, Peng Wang, and Yanning Zhang. VadCLIP: Adapting vision-language models for weakly supervised video anomaly detection. In *AAAI*, 2024. 2
- [21] Yajun Xu et al. TAD: A large-scale benchmark for traffic accidents detection from video surveillance. *arXiv preprint arXiv:2209.12386*, 2022. 2
- [22] Yu Yao, Xizi Wang, Mingze Xu, Zelin Pu, Ella Atkins, and David Crandall. DoTA: Unsupervised detection of traffic anomaly in driving videos. *IEEE TPAMI*, 2022. 2
- [23] Luca Zanella, Willi Menapace, Massimiliano Mancini, Yiming Wang, and Elisa Ricci. Harnessing large language models for training-free video anomaly detection. In *CVPR*, 2024. 2
- [24] Qihang Zhou, Guansong Pang, Yu Tian, Shibo He, and Jiming Chen. AnomalyCLIP: Object-agnostic prompt learning for zero-shot anomaly detection. In *ICLR*, 2024. 2

A. Prompts

All three prompts are reproduced verbatim. Model API snapshots used for submission: qwen3-vl-plus (Alibaba DashScope, April 2026 endpoint dashscope-us), gemini-3.1-flash-lite-preview (Google Gemini API, April 2026 snapshot; since promoted to general availability as gemini-3.1-flash-lite [6]). Temperature is 0.1 for all calls, max.tokens= 256 for Qwen passes, 1024 for Gemini typing.

A.1. Pass 1 (Qwen3-VL, coarse T+S+C)

This is a traffic surveillance video sampled at 1 frame per second. Frame numbers correspond to seconds in the video (frame 0 = 0s, frame 1 = 1s, ...). The video duration is {duration} seconds.

A traffic accident occurs in this video. Please analyze carefully and answer:

1. Time: At what second does the collision or accident impact occur?
2. Location: Point to the exact location in the frame where the impact happens. Return coordinates as values between 0 and 1000,

where (0,0) is top-left and (1000,1000) is bottom-right of the frame.

3. Type: head-on, rear-end, t-bone, sideswipe, or single.

Return ONLY a JSON object:

```
{"time": <seconds>, "x": <0-1000>, "y": <0-1000>, "type": "<type>"}
```

A.2. Pass 2 (Qwen3-VL, fine T+S)

These frames are extracted at 5 frames per second from a traffic surveillance video. Each frame is labeled with its precise timestamp. The time window shown is from {start}s to {end}s.

A traffic accident occurs somewhere in this video. If the collision happens within this time window, identify:

1. Exact time: The precise moment (to 0.1 second) of collision or impact.
2. Exact location: The impact point, as coordinates between 0 and 1000.

If you cannot see a collision in these frames, return time as -1.

Return ONLY a JSON object:

```
{"time": <seconds with 1 decimal or -1>, "x": <0-1000>, "y": <0-1000>}
```

A.3. Type Classification (Gemini 3.1)

A traffic collision HAS occurred in this surveillance clip. You MUST classify its type. This clip shows ~6 seconds leading up to and including the collision moment.

Collision types - pick exactly ONE:

- head_on: Two vehicles approach from OPPOSITE directions, collide front-to-front.
- rear_end: Two vehicles travel SAME direction; trailing one hits leading one from behind.
- t_bone: One vehicle strikes the SIDE of another at roughly 90 degrees.
- sideswipe: Two vehicles in parallel lanes make lateral/glancing contact.
- single: Only ONE vehicle involved.

Watch vehicle MOTION carefully across the clip. You MUST pick the most likely type.

B. Reproducibility & Cost

- **API cost** (April 2026): Pass 1 ~\$4, Pass 2 ~\$6, Gemini typing ~\$10. Total ~\$20 on 2,027 videos (~\$0.01/video).
- **Wall-clock**: ~100 minutes at 5 workers for Pass 1; ~180 minutes at 5 workers for Pass 2; ~15 minutes at 10 workers for Gemini. Total ~5 hours on a consumer workstation with a single residential network connection.

- **Hyperparameters** were fixed during development by inspection of the 2,211 CARLA synthetic dev videos and a small debug sample of public Kaggle dev-split real videos. Values: $\Delta=3$ s window, $\tau=0.3$ s temporal boundary tolerance, $m=10$ spatial margin on the $[0, 1000]^2$ grid, $2.5\times$ type-clip crop. **No grid search was performed on the 2,027 real test videos**; sensitivity to ± 1 -step perturbations of τ and m is ≤ 0.002 in ACC^S (Appendix C).

- **Physics fallback** used on Pass 1 API failures (17%) is YOLO26x + ByteTrack + multi-channel physics scoring. Its scorer weights (approach, IoU-surge, sustained-IoU, interaction-bias) were grid-searched on a 100-video CARLA sim split during challenge development and frozen before the real-test labels were released.

- **Data provenance**. Ground-truth annotations for the 2,027 real test videos were released publicly by the ACCIDENT benchmark organizers on Kaggle after the competition ended (<https://www.kaggle.com/datasets/picekl/accident>). We use them only for evaluation and post-hoc failure analysis. All pipeline hyperparameters and prompts were frozen before this release.

- **Artifact release**. To support reproducibility under API drift, we will release per-video raw VLM JSON outputs and parsed prediction CSVs alongside the camera-ready code.

- **Evaluation script** mirrors the public leaderboard’s convention: $\sigma_t=1$ s Gaussian temporal similarity; global mean GT bbox width and height ($\sigma_x=0.127$, $\sigma_y=0.119$) for spatial; Top-1 accuracy for type; harmonic mean combines the three.

- **Challenge compliance**. ACCIDENT@CVPR 2026 is an open prediction-file competition (participants upload a per-video CSV; it is not a sandboxed, compute-capped code competition), and its sole learning constraint is the prohibition on training or fine-tuning on labeled real accident footage. Our pipeline meets this: every model is frozen and used zero-shot. The challenge places no restriction on publicly available pretrained models or external inference services – the organizers’ own baselines use pretrained optical flow and CLIP [11, 14]. Both APIs we invoke, Qwen3-VL-Plus (Alibaba DashScope) and Gemini 3.1 Flash-Lite (Google) [1, 6], were publicly released, documented, and equally accessible to any participant under standard pay-as-you-go commercial terms throughout the submission window (April 2026), at a total cost of ~\$20 for the full 2,027-video test set. We use no private models, privileged endpoints, or non-public data.

C. Hyperparameter Sensitivity

This is a post-hoc analysis. The numbers in Table 3 were computed on the publicly-released test labels *after* the competition closed and were *not* used for hyperparameter selection. Defaults $\tau=0.3$ s and $m=10$ were fixed by inspection

on the 2,211 CARLA development videos and frozen before the labels were released (App. B). Each threshold is swept while the other is held at its default to assess robustness. Table 3. Sensitivity of ACC^S to the two gate thresholds on 2,027 real test videos ($\sigma_t=1$). Defaults marked with \star .

τ (s)	T	S	C	ACC^S	m	T	S	C	ACC^S
0.1	0.497	0.538	0.591	0.5393	0	0.497	0.462	0.591	0.5113
0.2	0.497	0.538	0.591	0.5393	5	0.497	0.538	0.591	0.5393
\star 0.3	0.497	0.538	0.591	0.5393	\star 10	0.497	0.538	0.591	0.5393
0.5	0.496	0.538	0.591	0.5385	20	0.497	0.538	0.591	0.5393
1.0	0.494	0.538	0.591	0.5377	50	0.497	0.538	0.591	0.5392

τ is effectively flat in $[0.1, 0.3]$ and degrades by only $\Delta ACC^S \leq 0.002$ even at $\tau=1.0$ s – Pass 2’s boundary-hedge detection (returning exact window endpoints) is sharp enough that the tolerance window has negligible effect. In contrast, m has one critical transition at $m=0$: disabling the margin admits Qwen-returned invalid-coordinate responses (raw -1 , after $/1000$ normalization becomes -0.001) and costs $\Delta S = -0.076$. Any positive margin in $[5, 50]$ is equivalent. Neither hyperparameter is knife-edge, and the CARLA-tuned values transfer to real data without any re-tuning on the released test labels.

D. Fallback Contribution Analysis

Pass 1 API failures trigger a fallback to the YOLO26x + ByteTrack + multi-channel physics scorer for 346 videos (17.1% of the test split). Table 4 decomposes the final $ACC^S=0.539$ by subset.

Table 4. Fallback contribution to the final score. VLM-success rows receive Pass 1+Pass 2 Qwen3-VL grounding and Gemini type; fallback rows use YOLO+physics for (t, x, y, c) . “Naive-fill” replaces the 346 fallback rows with trivial defaults (midpoint time, image center, majority type *single*) to estimate a pure-VLM ceiling with no informative fallback.

Subset	N	T	S	C	ACC^S
Pass 1 VLM success	1681	0.525	0.553	0.590	0.554
Pass 1 fallback (physics)	346	0.366	0.464	0.595	0.457
Full submission (ours)	2027	0.497	0.538	0.591	0.539
VLM + naive-fill fallback	2027	0.466	0.499	0.543	0.501

Three observations: **(i)** The VLM subset alone scores 0.554, above the full submission – confirming VLM is the dominant signal. **(ii)** The fallback subset still scores 0.457, well above all Kaggle public baselines (Optical Flow 0.251, BBox Dynamics 0.270, Naive 0.289) and Molmo-7B (0.396); the physics fallback is not a weak baseline. **(iii)** If we replace the 346 fallback rows with trivial naive defaults, ACC^S drops to 0.501 – still above the benchmark paper’s best-of-baselines oracle (0.412). This isolates the contribution of the VLM pipeline from the fallback heuristic. Failure rate is roughly uniform across duration buckets, day/night, weather, quality, and resolution (each cell: 12–22%), so the fallback is not concentrated on a particular failure mode.

E. Per-Type Breakdown

Table 5. Per-type performance of our full pipeline at $\sigma_t=1$. Head-on and sideswipe fail on type alone; their T and S components are healthy. Pooled $ACC^S=0.539$ differs from the weighted mean due to harmonic-mean non-linearity.

GT type	N	T	S	C	ACC^S
head-on	117	0.633	0.637	0.043	0.113
rear-end	328	0.451	0.553	0.582	0.522
sideswipe	245	0.442	0.454	0.057	0.137
t-bone	657	0.661	0.623	0.836	0.695
single	680	0.359	0.462	0.644	0.461

F. Ethics and Deployment

The pipeline routes CCTV footage through third-party commercial VLM APIs. For production deployment, public-facing surveillance clips must be handled under the camera operator’s data-use agreement, and any on-route personally identifiable information (faces, license plates) should be redacted prior to upload. The failure-mode analysis (Sec. 4.4) quantifies residual temporal ambiguity (median 1.1 s Pass 2 MAE; 10% tail beyond 10 s) that is not yet acceptable for first-notice-of-loss (FNOL) automation without a human-in-the-loop gate. All three prompts (App. A) assume *a priori* that an accident is present – valid for this benchmark, but in open-world deployment this closed-world framing must be replaced by an upstream binary detector (or the human-in-the-loop gate above) before grounding is trusted. Head-on and sideswipe classes have very low per-class accuracy (≤ 0.14) and should not be trusted unaided.